

Site Specific Electropolymerization To Form Transition-Metal-Containing, Electroactive Polythiophenes

Jerry L. Reddinger and John R. Reynolds*

Center for Macromolecular Science and Engineering, Department of Chemistry,
University of Florida, Gainesville, Florida 32611

Received August 19, 1997. Revised Manuscript Received February 6, 1998

We report a series of novel bis(salicylidene) metal complexes that undergo oxidative electropolymerization to afford polymers comprised of three different backbone constitutions and a variety of film colors. The ligand architecture, being either *N,N*-bis(salicylidene)-3,4-diaminothiophene (SALOTH) or *N,N*-bis(salicylidene)-3',4'-diamino-2,2':5',2''-terthiophene (BTh-SALOTH), is based upon a thiophene or 2,2':5',2''-terthiophene core with the imine functionalities attached at the 3-, 4-, or 3',4'-positions, respectively. This monomer design possesses two switchable polymerization sites that yield phenylene-linked backbones with unblocked salicylidene rings or polythiophenes with the use of methyl blocking groups. As expected with metal centers in direct electronic communication with the polymer chains, the metal type has a dramatic influence over electrochromic properties, with colors unique to each metal being achieved. For example, the Ni-containing films exhibit an orange-to-green redox transition while the Cu-containing analogues display a light green/dark green pair. Details of monomer synthesis as well as full electrochemical details for the monomers and polymers are presented.

Introduction

The field of conducting and electroactive polymers continues to expand with the advent of new systems suitable for an ever-growing myriad of applications that include corrosion protection, electrochromics, chemical sensors, and batteries, along with ESD and EMI-shielding materials.¹ More specifically, in the past few years, there has been an increase in synthetic efforts aimed at obtaining metal-containing, conducting polymers, and these materials suggest an array of potential uses (e.g., electrocatalysis, electrochromic displays, and molecular recognition). There are many examples of π -conjugated polymers in the literature that possess pendant metal centers, attached to the backbone by insulating tethers.² For the most part metal/polymer interactions in these systems are inherently weak. Thus, to maximize the interaction of metal centers with the polymer's extended π -system, the ideal structure would have the metal centers directly affixed to, and in direct electronic communication with, the polymer backbone.

As yet, there are still only a few reported examples of conducting and electroactive polymers where metal centers are in conjugation with the polymer's π -system.^{3–7} All of these systems possess metal centers coordinated to bidentate, nitrogen-containing, heterocyclic units

(2,2'-bithiazole or 2,2'-bipyridyl) incorporated into the polymer backbone. While the number of examples are few, these preliminary efforts have already shown the broad flexibility that metal coordination can impart to traditional organic systems. Peng and Yu have utilized the conjugated backbone of ruthenium-containing polymers to enhance the photosensitivity of the parent organic polymer.⁵ Such an effect is important for the future development of photoconductive materials. Zhu and Swager have used metal/polymer complexation as a means to polyrotaxane formation via a Sauvage-type⁸ template effect.^{6b} Wang and Wasielewski have shown the sensitivity of a pseudo-poly(phenylenevinylene) system to the complexation of various metal ions.⁷ Their work utilized conformational changes of the polymer that are associated with the coordination of the metal ions, affording a system that can toggle between its conjugated and nonconjugated forms.

Our group has reported on a number of low-oxidation-potential thiophene-based monomers that when polymerized form electroactive materials possessing novel electronic properties.⁹ We have recently reported on our initial efforts to tune the optical and electronic properties of polymers via the incorporation of metal centers.¹⁰

(1) For an up-to-date overview, see the Proceeding of ICSM 1996, *Synth. Met.* **1997**, 84–87, and *Handbook of Conducting Polymers*, 2nd ed., T. A. Skotheim, R. L. Elsenbaumer, and J. R. Reynolds, Eds., Marcel Dekker: New York, 1998.

(2) For example see: (a) Deronzier, A.; Moutet, J.-C. *Acc. Chem. Res.* **1989**, 22, 255. (b) Zotti, G.; Zecchin, S.; Schiavon, G.; Berlin, A.; Pagani, G.; Canavesi, A. *Chem. Mater.* **1995**, 7, 2309.

(3) (a) Yamamoto, T.; Maruyama, T.; Zhou, Z.-H.; Ito, T.; Fukuda, T.; Yoneda, Y.; Begum, F.; Ikeda, T.; Sasaki, S.; Takezoe, H.; Fukuda, A.; Kubota, K. *J. Am. Chem. Soc.* **1994**, 116, 4832. (b) Maruyama, T.; Yamamoto, T. *Inorg. Chim. Acta* **1995**, 238, 9.

(4) Wolf, M. O.; Wrighton, M. S. *Chem. Mater.* **1994**, 6, 1526.

(5) Peng, Z.; Yu, L. *J. Am. Chem. Soc.* **1996**, 118, 3777.

(6) (a) Zhu, S.; Swager, T. M. *Adv. Mater.* **1996**, 8, 497. (b) Zhu, S.; Carroll, P. J.; Swager, T. M. *J. Am. Chem. Soc.* **1996**, 118, 8713.

(7) Wang, B.; Wasielewski, M. R. *J. Am. Chem. Soc.* **1997**, 119, 12.

(8) Sauvage, J. P. *Acc. Chem. Res.* **1990**, 23, 321.

In our initial efforts, our work was geared toward electrochromic applications for the subsequent construction of dual-polymer electrochromic devices,^{9h} but we have also found such systems to make excellent polymeric sensors of both ionic and neutral species.¹¹

One of the key limitations of polymer-based electrochromic devices is that of device lifetime, and it has been shown that chemical compatibility between device components greatly enhances both durability and performance. This compatibility is most directly accomplished by using polymers possessing very similar structures, and thus, the introduction of metal centers into polymeric architectures that have already proven to be useful candidates for device construction, could afford a highly compatible material possessing the ability to be tuned over a wide color range.

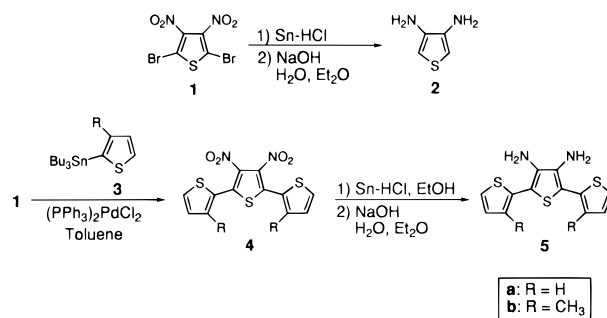
Results and Discussion

Monomer Synthesis. Given our background in electrochromic materials, and the requirements for the successful incorporation of transition metals into conducting polymers, we elected to append a tetradentate coordinating bis(salicylidene)-type ligand onto a thiophene core functionalized with various heterocyclic substituents. The Schiff base ligand system was selected given its typically facile synthesis, ability to coordinate a broad range of transition metals, and their resistance to decomplexation under a variety of harsh conditions.¹² Thiophene is an extremely well suited nucleus for the macrocyclic ligand as it affords a number of synthetic options for further derivatization. More specifically, by leaving the more reactive 2- and 5-sites open, the subsequent coupling of other thienyl ring systems yields further derivatives, more susceptible to electrochemical polymerization.

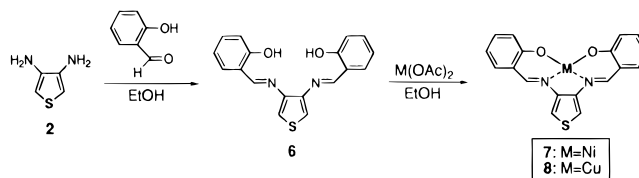
The key precursors required for the formation of these types of bis(salicylidene) ligands are the 3,4-diaminothiophenes, which we prepared as shown in Scheme 1. Regardless of end target, 2,5-dibromo-3,4-dinitrothiophene¹³ (**1**), which can be prepared easily on the molar scale, was used as the starting material for the respective syntheses. Using the procedure developed by Outurquin and Paulmier, **1** was directly converted to the diamine **2** using a tin-mediated concomitant reduction/destannylation.¹⁴

A logical step in our monomer syntheses was to extend the effective conjugation length of the monomers,

Scheme 1



Scheme 2



and this is easily done by moving to a terheterocyclic core. Work in our laboratories⁹ and others¹⁵ has shown the benefits of using multiring monomers to decrease polymerization potential and better stabilize the oxidized species. The lowering of the polymerization potentials is paramount as it helps to suppress unwanted side reactions such as β -coupling and polymer degradation. Accordingly, we found **1** to readily undergo Pd-catalyzed cross coupling¹⁶ with various trialkylstannylthiophenes affording the dinitro-substituted terheterocyclic compounds **4a** and **4b**. We found that the use of toluene as opposed to other lower boiling, yet more polar solvents, gave higher yields in conjunction with shorter reaction times. Hence, upon purification via column chromatography, the terheterocyclic derivatives were obtained in 75–85% yields based on **1**. These dinitro species were then reduced using a modification of the procedure used for the reduction of **1**. With **4a** and **4b**, longer reaction times, along with the use of EtOH as cosolvent, were required for complete reduction to the corresponding diamines **5a** and **5b**.

The ligand *N,N*-bis(salicylidene)-3,4-diaminothiophene (SALOTH, **6**) was synthesized, as outlined in Scheme 2, via the condensation of salicylaldehyde with **2** and purified by recrystallization from EtOH. The subsequent complexation of **6** was achieved by addition of the ligand, dissolved in a hot ethanolic solution, to nickel or copper acetate in hot ethanol, and subsequent cooling afforded microcrystals of the target metal complexes **7** and **8** in moderate yields. The corresponding yields for both ligand formation and complexation were unexpectedly low (<35% combined yield), which we feel is attributable to the fact that the uncomplexed ligand is somewhat unstable in solution. To circumvent these complications, we opted to prepare subsequent complexes by the more direct route^{12c} of first combining the

(9) (a) Reynolds, J. R.; Child, A. D.; Ruiz, J. P.; Hong, S. Y.; Marynick, D. S. *Macromolecules* **1993**, *26*, 2095. (b) Reynolds, J. R.; Katritzky, A. R.; Soloducho, J.; Belyakov, S.; Sotzing, G.; Pyo, M. *Macromolecules* **1994**, *27*, 7225. (c) Child, A. D.; Sankaran, B.; Larmat, F.; Reynolds, J. R. *Macromolecules* **1995**, *28*, 6571. (d) Sotzing, G. A.; Reynolds, J. R. *J. Chem. Soc., Chem. Commun.* **1995**, 703. (e) Sotzing, G. A.; Reynolds, J. R.; Katritzky, A. R.; Soloducho, J.; Belyakov, S.; Musgrave, R. *Macromolecules* **1996**, *29*, 1679. (f) Sotzing, G. A.; Reynolds, J. R.; Steel, P. J. *Chem. Mater.* **1996**, *8*, 882. (g) Reddinger, J. L.; Sotzing, G. A.; Reynolds, J. R. *J. Chem. Soc., Chem. Commun.* **1996**, 1777. (h) Sapp, S. A.; Sotzing, G. A.; Reddinger, J. L.; Reynolds, J. R. *Adv. Mater.* **1996**, *8*, 808.

(10) Reddinger, J. L.; Reynolds, J. R. *Macromolecules* **1997**, *30*, 673.

(11) Reddinger, J. L.; Reynolds, J. R. *Chem. Mater.* **1998**, *10*, 3.

(12) (a) Wilkinson, G.; Gillard, R. D.; McCleverty, J. A., Eds. *Comprehensive Coordination Chemistry*; Pergamon Press: Oxford, 1987; Vol. 3. (b) *Ibid.*, Vol. 5. (c) Holm, R. H.; Everret, G. W.; Charkavorty, A. *Prog. Inorg. Chem.* **1966**, *7*, 83. (d) Marvel, C. S.; Aspey, A. A.; Dudley, E. A. *J. Am. Chem. Soc.* **1956**, *78*, 4905.

(13) Mozingo, R.; Harris, S. A.; Wolf, D. E.; Hoffhine, Jr., C. E.; Easton, N. E.; Folkers, K. *J. Am. Chem. Soc.* **1945**, *67*, 2092.

(14) Outurquin, F.; Paulmier, C. *Bull. Soc. Chim. Fr.* **1983**, *2*, 153.

(15) (a) Ferraris, J. P.; Skiles, G. D. *Polymer* **1987**, *28*, 179. (b) Ferraris, J. P.; Andrus, R. G.; Hrcncir, D. C. *J. Chem. Soc., Chem. Commun.* **1989**, 1318. (c) Pelter, A.; Maud, J. M.; Jenkins, I.; Sadeka, C.; Coles, G. *Tetrahedron Lett.* **1989**, *30*, 3461. (d) Roncali, J.; Gorgues, A.; Jubault, M. *Chem. Mater.* **1993**, *5*, 1456. (e) Lorcy, D.; Cava, M. P. *Adv. Mater.* **1992**, *4*, 562.

(16) Stille, J. K. *Angew. Chem., Int. Ed. Engl.* **1986**, *25*, 508.

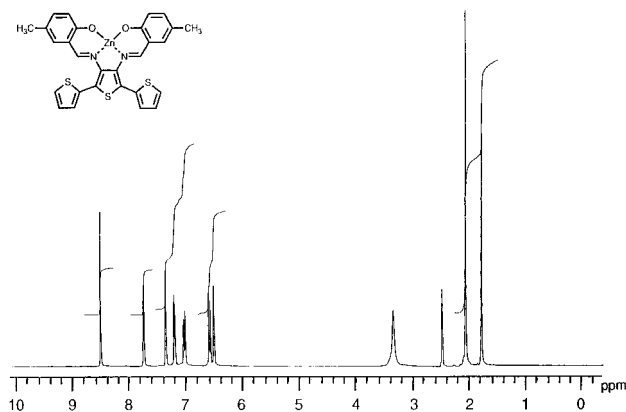
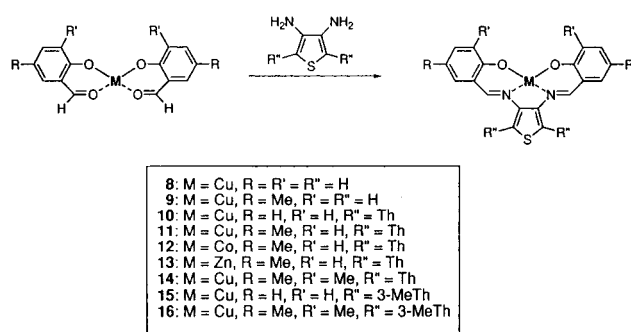


Figure 1. ^1H NMR spectrum for **13** in DMSO showing evidence for the presence of coordinated H_2O . The symmetrical nature of the aromatic portion of the spectrum is consistent with a coplanar arrangement of metal center and ligand core in the compound.

Scheme 3



salicylaldehyde and metal acetate and then condensing the resulting species with the corresponding diamine as shown in Scheme 3, with improved yields typically ranging from 65% to 85%. In this manner we prepared the broad family of monomers **8–16**.

Structural characterization, derived from elemental analyses and NMR spectroscopy, proved consistent with the complexed ligands. With the exception of the nickel complexes, combustion analysis showed all other monomers to contain varied amounts of H_2O . Extended periods of time (2–3 days) in a vacuum oven at elevated temperatures did not effect removal of this H_2O . When possible, ^1H NMR spectra were acquired and were in agreement with the expected structures. More detailed analysis of the NMR data was carried out in hopes of delineating the nature of the “coordinated” H_2O and other structural features. As shown in Figure 1, the ^1H NMR of **13** indicates that the monomer is highly symmetric (in DMSO at 20 °C) and includes approximately one coordinated H_2O molecule. Both the salicylidene protons and those of the terminal thiophene rings appear equivalent for the two respective halves of the molecule. This is consistent with a proposed pseudo- C_{2v} symmetry expected to be possessed by SALOTH complexes where the ligand/metal core can adopt a planar arrangement. (The ^{13}C NMR spectrum also shows similar evidence for this geometry by the simplicity of the resonances observed.) We had hoped for more definite structural information, but unfortunately, due to persistent twinning, crystals suitable for X-ray structure determination could not be obtained.

Table 1. Colors and Primary Electronic Absorptions for the SALOTH-Based Monomers

monomer	color	λ_{max} for primary electronic absorptions ^a
6	red/orange	270, 339
7	red/brown	265, 294, 309, 327, 365, 464, 483
8	green	243, 265, 308, 320, 337 (sh), 416
9	yellow/green	253, 271, 313, 325, 339, 430
10	dark green	250 (sh), 305, 422
11	dark green	257 (sh), 308, 440
12	brown	337, 432
13	bright yellow	249 (sh), 303, 404
14	dark green	261 (sh), 322, 442
15	brown/green	244 (sh), 309, 422
16	brown/green	241 (sh), 313, 435

^a Results obtained in CH_2Cl_2 at room temperature.

Electronic Spectra of Monomers. The electronic spectra for the various monomers in CH_2Cl_2 were obtained to provide insight into monomer geometry through the energies of metal-based transitions. Table 1 lists the principle features (listed as λ_{max}) present in the spectra for SALOTH **6** and monomers **7–16**. The absence of transitions above 500 nm is consistent with the proposed planar tetradentate core, as Ni^{2+} and Cu^{2+} environments of higher symmetry typically exhibit features in the 700–1500 nm range.

Comparison of the spectra of **6–8** shows that metal coordination results in the emergence of both metal-based transitions and blue shifts of the ligand-based absorptions. Such behavior is expected upon the coordination of ionic metal centers to unsaturated organic ligands. Furthermore, absorptions of the terheterocyclic complexes **11** and **14–16** are red shifted relative to **8** or **9**. This is also not surprising due to the extended conjugation possible with the multiring cores. However, this red shifting is significant from the standpoint that metal coordination does not completely disrupt the extended π -system present in the terthienyl derivatives. (As discussed later, this feature will become an important factor in the monomers' electrochemical behaviors.) When the spectra for the methyl-derivatized, bis(2-thienyl)SALOTH (BTh-Me₂SALOTH) ligand system coordinated with Co^{2+} , Cu^{2+} , or Zn^{2+} ions are compared, the absorptions for the Cu^{2+} derivative are found at the longest wavelengths with those of the Zn^{2+} complex occurring at the shortest wavelengths. This clearly shows that the metal centers are influencing the energies at which the ligand transitions occur. Hence, metal type should be a strong factor in determining the optical and electronic properties of the corresponding polymers, given the sensitive nature of their conjugated backbones.

Electropolymerization Results. To determine the possibility of electropolymerization, metal free-SALOTH **6** was investigated by cyclic voltammetry. A 5 mM CH_2Cl_2 solution containing 0.1 M tetrabutylammonium perchlorate electrolyte (TBAClO_4) was repeatedly scanned between -0.5 and $+0.9$ V versus Ag/Ag^+ (all further potentials will be referenced versus this reference electrode) at a scan rate of 100 mV/s, and the first three scans are shown in the top of Figure 2. The first scan for **6** possesses the greatest electroactivity while subsequent scans show a continued ebbing of current response. While the metal-free ligand **6** shows no such tendency to electropolymerize, the Ni-SALOTH com-

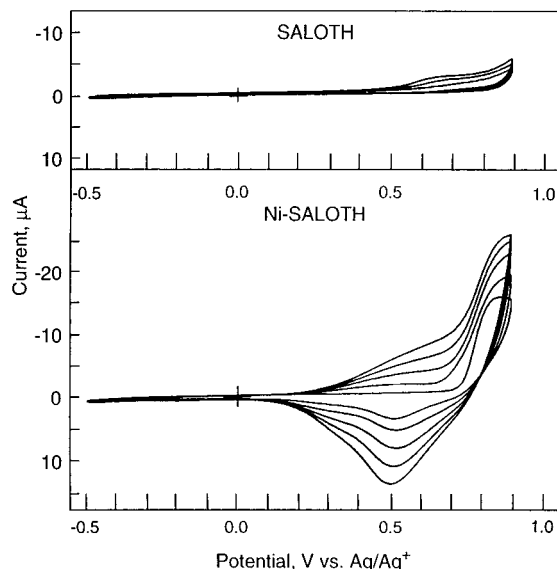


Figure 2. Repeated potential scans for **6** (top) and **7** (bottom). For **6**, the first scan shows the greatest electroactivity and subsequent cycling results in continued loss of electroactivity. Both experiments were conducted with 5 mM monomer in 0.1 M TBAClO₄/CH₂Cl₂ solutions, scanning anodically from -0.5 to +0.9 V at a scan rate of 100 mV/s.

plex **7** readily electropolymerizes under identical conditions to give polymer **7p**. The repeated potential scans for **7** are shown in the bottom of Figure 2. In contrast to the behavior exhibited by **6**, the first scan shows a sharp onset of monomer oxidation ($E_{\text{onset,m}}$) at +0.72 V and a reductive process ($E_{\text{p,c}}$) at +0.50 V. During the second scan, a new oxidation can be seen to grow in at +0.55 V, which is attributed to the oxidation of the newly formed polymer ($E_{\text{p,a}}$) and a marked increase in current response for monomer oxidation is evident. Continued scanning brings about further increases in electroactivity as well as the formation of a thick orange film on the electrode's surface. This increase in electroactivity is consistent with polymer film formation that possesses a larger surface area than the bare metal electrode.

For all of the different monomer types that were synthesized in this study, the copper complexes were significantly more soluble than the corresponding nickel analogues. (Solubility is important as more concentrated solutions tend to more readily undergo electropolymerization.) To avoid any spurious results that may occur due to poor solubility, only the copper series will be used to compare the properties of the various structure types. Those SALOTH derivatives for which both the resulting nickel and copper complexes were soluble exhibited similar tendencies to electropolymerize and gave voltammograms displaying similar shapes and features. The repeated potential growth voltammogram for Cu-SALOTH **8**, yielding polymer **8p**, using identical conditions as employed for the synthesis of **7p**, is shown in Figure 3. This monomer possessed an $E_{\text{onset,m}}$ of +0.75 V, an oxidation centered around +0.6 V, and $E_{\text{p,c}}$ at +0.57 V. While the potential values for the various processes are somewhat higher than those for the nickel complex, both polymerizations appear to proceed in a similar manner with relatively sharp onsets for monomer oxidation.

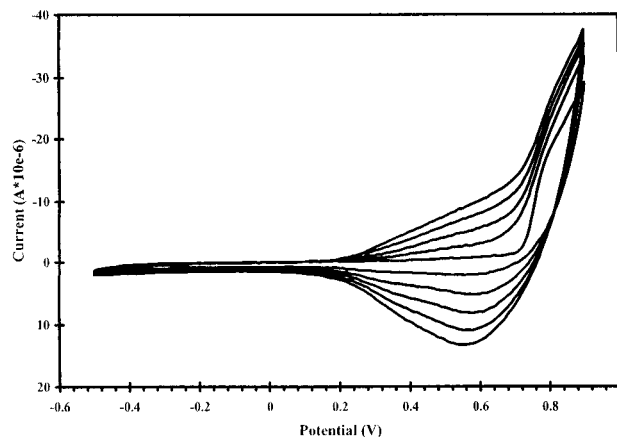


Figure 3. Electropolymerization of 5 mM **8** in 0.1 M TBAClO₄/CH₂Cl₂ solutions, scanning anodically from -0.5 to +0.9 V at a scan rate of 100 mV/s. The flat base current and ensuing sharp onset is indicative of the phenylene-linked polymers.

These results are in agreement with the reported electrochemical properties for various other bis(salicylidene) transition-metal complexes under oxidative conditions. Horwitz and Murray found that aniline-terminated Salen chelates formed polymer films upon oxidation of the metal center in CH₃CN-based electrolytes.¹⁷ Goldsby et al. later proposed a solvent-dependent mechanism for the oxidative polymerization of Ni(II) bis(salicylaldehyde) complexes.^{18a} Their postulation incorporated the fact that Ni(II) complexes can be reversibly oxidized in solvents with high donor numbers (DN; e.g., pyridine, DMF, DMSO) where the solvent can stabilize the oxidized metal center via axial ligation. However, solvents such as CH₃CN and CH₂Cl₂, possessing low DNs, can afford no enhanced stability through coordination to the metal and polymerization occurs. While the exact mechanism by which this polymerization occurs is unclear, it is believed that rapid internal electron transfer from metal to ligand is a key component. A number of other examples have since used this tendency of bis(salicylaldehyde) chelates to undergo oxidative polymerization when Mn, Co, Ni, Cu, or Zn are the complexed metals.¹⁷⁻²⁰ Audebert et al. have found evidence for Goldsby's presumption that these polymers consisted of phenylene linkages para to the phenolic carbon of the salicylidene rings by decomplexation/hydrolysis of a representative Ni-Salen polymer and subsequent characterization of the resulting material.²⁰

Given this precedence and the steric congestion surrounding the thiophene core in complexes **7** and **8**, we felt it rather unlikely that the corresponding polymers **7p** and **8p** possessed polythiophene backbones. To ascertain which polymerization mode was operating, we elected to block the key positions of the salicylidene rings to prevent polymerization at those sites. Elec-

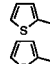
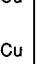
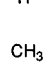
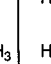
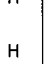
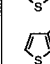
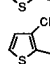
(17) Horwitz, C. P.; Murray, R. W. *Mol. Cryst. Liq. Cryst.* **1988**, *160*, 389.

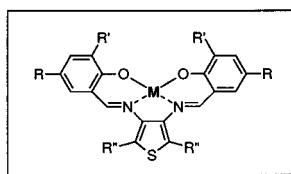
(18) (a) Goldsby, K. A.; Blaho, J. K.; Hoferkamp, L. A. *Polyhedron* **1989**, *8*, 113. (b) Hoferkamp, L. A.; Goldsby, K. A. *Chem. Mater.* **1989**, *1*, 348.

(19) Bedioui, F.; Labbe, E.; Gutierrez-Granados, S.; Devynck, J. J. *Electroanal. Chem.* **1991**, *301*, 267.

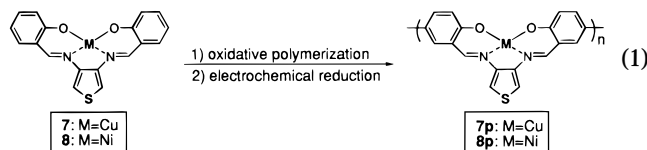
(20) (a) Audebert, P.; Capdevielle, P.; Maumy, M. *New J. Chem.* **1992**, *16*, 697. (b) Capdevielle, P.; Maumy, M.; Audebert, P.; Plaza, B. *New J. Chem.* **1994**, *18*, 519.

Table 2. SALOTH-Based Monomer Structures and Their Corresponding Electropolymerization Behavior Including Polymer Linkage

Compound	M	R	R'	R''	Polymer	Linkage
6	-	H	H	H	No	-
7	Ni	H	H	H	Yes	Phenylene
8	Cu	H	H	H	Yes	Phenylene
9	Cu	CH ₃	H	H	No	-
10	Cu	H	H		Yes	Mixture
11	Cu	CH ₃	H		Yes	Thienylene
12	Co	CH ₃	H		Yes	Thienylene
13	Zn	CH ₃	H		Yes	Thienylene
14	Cu	CH ₃	CH ₃		Yes	Thienylene
15	Cu	H	H		Yes	Phenylene
16	Cu	CH ₃	H		No	-



tropolymerization for complex **9** failed, as expected, strongly suggesting that polymers **7p** and **8p** were comprised exclusively of phenylene linkages as depicted by eq 1 and overviewed in Table 2 (including the type of linkage formed during electropolymerization).



When the monomer is of the extended conjugation motif (possessing a multiring core), however, there exists the possibility for thienylene linkages to occur in addition to the previously encountered phenylene couplings. Indeed, Cu-BTh-SALOTH (**10**) likely gives a mixture of coupling types, although polymerization occurs approximately 100 mV higher than for Cu-SALOTH. A 5 mM solution of **10** in 0.1 M TBAClO₄/CH₂Cl₂ was cycled between -0.3 and +1.05 V. While its behavior modeled that of its less conjugated analogue, higher potentials were recorded for all of the electrochemical processes with $E_{\text{onset,m}}$, $E_{\text{p,a}}$, and $E_{\text{p,c}}$ occurring at +0.83, +0.72, and +0.68 V, respectively.

Analogous blocking techniques, as employed in the synthesis of **9**, were the impetus for the synthesis of Cu-BTh-Me₂SALOTH (**11**) and Cu-BTh-Me₄SALOTH (**14**), where such functionalization would force the ultimate polymerization sites to those of the terminal thiophene rings of the terthiophene core. Repeated potential cycling of a 5 mM solution of **11** in 0.1 M TBAClO₄/CH₂Cl₂ between -0.3 and +1.05 V at a scan rate of 100 mV/s showed direct evidence of electropolymerization to polymer **11p** along with film formation upon the electrode's surface. The resulting voltammogram, shown in Figure 4, possesses two features not seen with the other monomers, namely, an unresolved

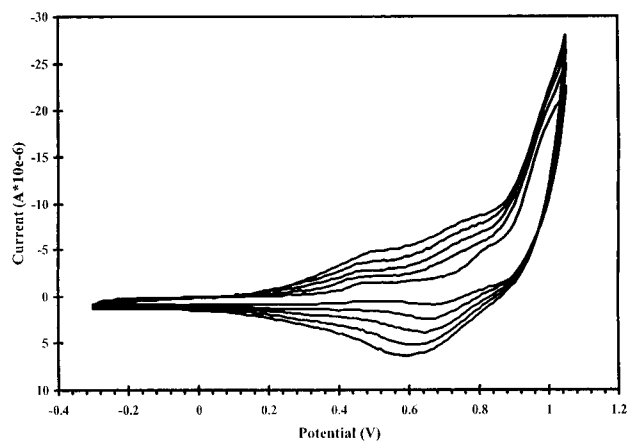
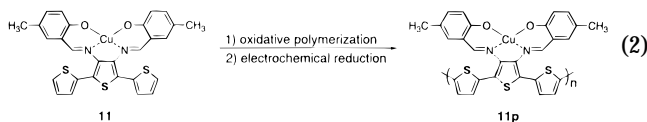


Figure 4. Repeated potential scanning polymerization of 5 mM **11** in 0.1 M TBAClO₄/CH₂Cl₂ solutions, scanning anodically from -0.3 to +1.05 V at a scan rate of 100 mV/s. Low potential features (~0.4 V) and a broad, sloping onset were discovered for all polythiophene-forming monomers.

peak is observed at ca. +0.4 V and a broad, sloping onset prior to metal oxidation above +0.8 V. We attribute this "low potential" feature to the growing polythiophene backbone.²¹ Hence, we find that polymers **11p** and **14p** are formed from these "blocked", extended-conjugation monomers via a transition-metal-assisted polymerization and possess the structure type shown in eq 2. Similar behavior to **11** was found for **12** and **13**, indicating the metal type does not inhibit electropolymerization.



To further test our proposed system for detecting the switching of the ultimate polymerization sites of the SALOTH system by voltammogram shape, we synthesized the monomers **15** and **16** and subjected them to electrochemical oxidation. A previous report has shown the reluctance of various 3,3'-dialkyl-3',4'-diimino-2,2':5',2''-terthiophenes to undergo electropolymerization.²² Thus, with monomer **15** electropolymerization should, and did, occur to yield a phenylene-linked polymer. The voltammograms possessed the characteristic sharp onset that we have attributed to coupling via phenylene linkages. Finally, the attempt to electropolymerize **16** was, in effect, a negative experiment as polymerization should be completely stopped due to the blocking of salicylidene sites. As expected, **16** did not polymerize upon exposure to oxidizing potentials. While voltammograms showed the irreversible metal/ligand oxidation, no growth was evident nor was film formed on the electrode.

Polymer Electrochemistry. All of the films studied in this work were found to be very robust, requiring the use of abrasive pads for their removal from platinum buttons. The electrochemical behavior of the polymer

(21) We have attempted electropolymerization at potentials too low to access the metal-centered redox processes, but film growth was extremely slow.

(22) Kitamura, C.; Tanaka, S.; Yamashita, Y. *Chem. Mater.* **1996**, *8*, 570.

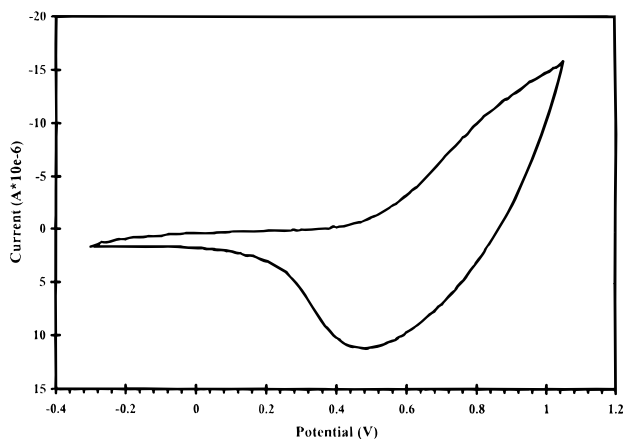


Figure 5. Cyclic voltammogram for polymer **8p**, grown on a platinum button, with anodic scanning between -0.3 and $+1.0$ V at a scan rate of 100 mV/s.

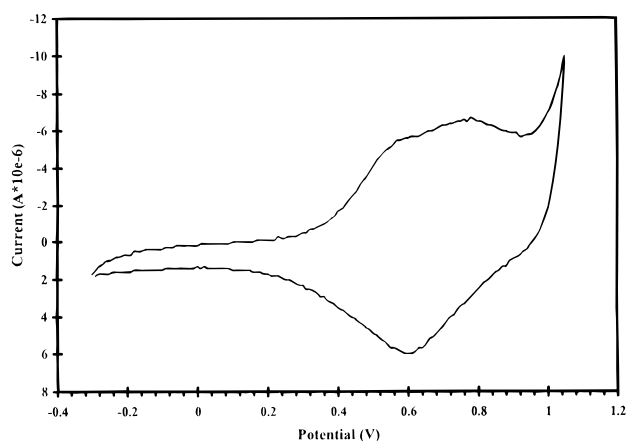


Figure 6. Polymer cyclic voltammogram for a film of **11p** on a platinum button under anodic scanning from -0.3 to $+1.0$ V at a scan rate of 100 mV/s.

films were probed using cyclic voltammetry and a representative voltammogram for the phenylene-linked polymer **8p** is shown in Figure 5. Upon rinsing and equilibrating freshly grown films in monomer-free 0.1 M TBAClO₄-CH₂Cl₂, the films were precycled for five scans between -0.5 and $+1.05$ V. Anodic scanning showed a broad, indistinct oxidation with onset around $+0.5$ V and a single reduction ($E_{p,c}$ at $+0.71$ V). The scan rate dependency of the film, using scan rates from 25 to 400 mV/s, revealed a linear relationship between the square root of scan rate and peak current. This behavior implies that the associated redox processes are diffusion-limited.

Polymer cyclic voltammograms of the thienylene-linked **11p**, such as that shown in Figure 6, appeared quite different from those of the phenylene-linked polymers. Most interesting is the appearance of two anodic processes seen at low scan rates (≤ 100 mV/s). At a scan rate of 50 mV/s, the first process, which occurs at a potential lower than in the previous polymers ($E_{p1,a}$ at 0.4 V), is likely that of thiophene backbone and the second ($E_{p2,a}$ at $+0.6$ V) being metal/ligand-based. (Table 3 lists the redox potential values for all monomers and polymers studied.) The effect of scan rate on the voltammograms of the polymer films of **11p** was investigated as above and is shown in Figure 7. Much like that noted for the phenylene-linked systems, a

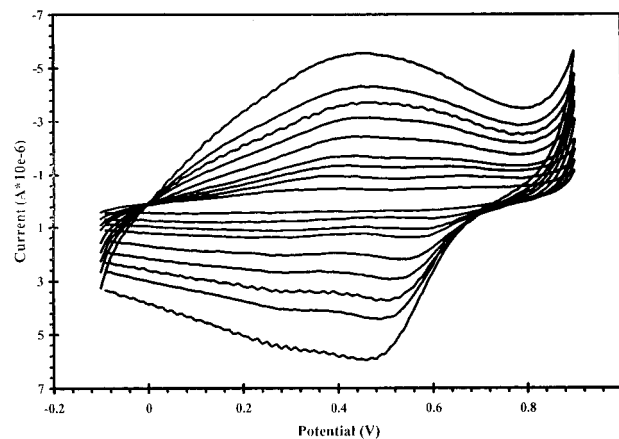


Figure 7. Scan rate dependence of a film of polymer **11p** on a platinum button electrode. Scan rates were 25 (innermost), 50 , 75 , 100 , 125 , 150 , 200 , 250 , 300 , and 400 mV/s (outermost). As with polymer **8p**, peak current was found to scale linearly with the square root of scan rate.

Table 3. Electrochemical Results for the Redox Processes Exhibited by the SALOTH-Based Monomers and Their Corresponding Polymers

monomer	redox process			polymer	redox process	
	E_{onset}	$E_{p,m}$	$E_{p,c}$		$E_{p,a}$	$E_{p,c}$
6	+0.57	+0.94				
7	+0.72	+0.83	+0.50	7p	+0.79	+0.47
8	+0.75	+0.89	+0.45	8p	+0.84	+0.69
9	+0.73	+0.88				
10	+0.83	+0.90	+0.68	10p	+0.64	+0.54
					+0.85	+0.68
11	+0.38	+0.99	+0.53	11p	+0.64	+0.59
					+0.78	
12	+0.16	+0.94	+0.32	12p	+0.65	+0.41
					+0.91	+0.81
13	+0.21	+0.84	+0.40	13p	+0.54	+0.31
14	+0.38	+0.98	+0.47	14p	+0.63	+0.57
					+0.78	
15	+0.72	+1.04	+0.68	15p	+0.82	+0.52
16	+0.71	+1.02				

linear relationship was found between the square root of scan rate and peak current for the thienylene backbone polymers.

Optoelectrochemistry. Optoelectrochemical analysis of the films was attempted to help elucidate the band structure of the polymers. For these experiments, films were grown on indium tin oxide-coated glass (ITO), which functions as a transparent electrode. A three-electrode cell was constructed in a typical quartz cuvette, and the UV-vis-NIR spectra recorded at various applied potentials. Performing such an experiment on classical conducting polymers is a very straightforward manner by which to monitor the emergence and growth of lower energy transitions (attributed to the formation of the polymer's polaronic and bipolaronic states) as the polymer is oxidized to its conducting form.

The presence of broad absorptions in the electronic spectra of these new systems greatly reduced the ability to observe distinct changes upon the stepping of applied potentials. Figure 8 shows the effect of applied potential on the electronic absorption of a film of **13p** grown on an ITO-coated slide. The growth of new transitions at lower energies with subsequent decrease of the higher energy absorption can be seen as the potential is stepped from -0.45 to $+0.87$ V. The relatively small overall

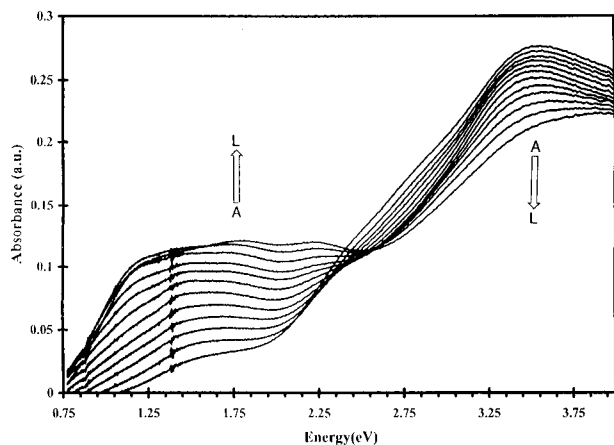


Figure 8. Optoelectrochemical investigation of a film of polymer **13p** grown on ITO-coated glass. Potentials for which spectra were taken are -0.20 (A), $+0.50$, $+0.60$, $+0.67$, $+0.73$, $+0.78$, $+0.83$, $+0.88$, $+0.93$, $+0.99$, $+1.05$, and $+1.12$ V (L). The higher energy transition continually decreased as the lower energy absorptions emerged and increased with increasing potentials.

decrease of the high energy absorption likely indicates a low doping level. Visually, one can observe a color change from translucent brown to a faint transparent green upon oxidation of the film.

Conclusion

We have developed a series of novel, metal-containing monomers that when electropolymerized yield electroactive polymers containing transition metal centers directly affixed to the conjugated backbone. A unique feature of this monomer architecture is that it possesses multiple polymerization sites that can be functionalized to selectively afford polymers comprised of phenylene- or thienylene-linkages or mixtures of the two. Furthermore, we have noticed a distinct difference in the shape of the first scan of voltammograms for the two different polymer types. The phenylene systems exhibit a smooth base current with a very sharp onset, as opposed to the presence of "low potential" features and broad, sloping onset found in the thienylene-linked systems. Our initial aim of this study was to investigate the possibility of using metal centers to modulate optical properties of conjugated polymers. We have seen, as in the case of polymers **7p** and **8p**, that metal type does in fact dictate electrochromic properties in these systems. We are now presently utilizing modification of this design for the fabrication of dual-metal ion-containing, polymeric sensors.

Experimental Section

Instrumentation. NMR spectra were obtained on a 300 MHz spectrometer with Me_4Si as internal standard and CDCl_3 (unless otherwise noted) as solvent. All melting points are uncorrected. All experiments involving the use of a potentiostat were performed on an EG&G Princeton Applied Research Model 273 potentiostat/galvanostat interfaced with EG&G Electrochemical software. Optoelectrochemical analysis was obtained using a Varian Cary 5E UV-vis-NIR spectrophotometer in conjunction with the aforementioned potentiostat. Mass spectral analyses were performed by the University of Florida Mass Spectral Services, Gainesville, FL. Elemental Analyses were performed by Robertson Microlabs, Madison, NJ.

Reagents. All reactions were performed under prepurified nitrogen or argon, using Schlenk-type techniques. Glassware was dried in an oven overnight or flame dried and then cooled under a stream of inert gas. The following compounds were synthesized using standard literature procedures: 2-(tributylstannyl)thiophene,²³ 2-(tributylstannyl)-3-methylthiophene,²³ 2,5-dibromothiophene,²⁴ 2,5-dibromo-3,4-dinitrothiophene,¹³ 3,4-diaminothiophene,¹⁴ 2-hydroxy-4-methylbenzaldehyde,²⁵ 2-hydroxy-4,6-dimethylbenzaldehyde.²⁵ Bis(triphenylphosphine)-palladium(II) chloride was prepared immediately before each coupling reaction by refluxing 1 equiv of palladium(II) chloride, 2.1 equiv of triphenylphosphine, and 2 equiv of lithium chloride in dry methanol for 1 h. Upon cooling, the solvent is removed by Schlenk filtration, and the resulting yellow solid dried in vacuo.

3',4'-Dinitro-2,2':5',2''-terthiophene (4a). To the round-bottomed flask containing the freshly made catalyst was added 2-(tributylstannyl)thiophene (3.51 g, 0.0094 mol), 2,5-dibromo-3,4-dinitrothiophene (1.53 g, 0.0092 mol), and dry toluene (60 mL). The reaction mixture was refluxed for 12 h, and the solvent removed by rotary evaporation. The residue was dissolved in CH_2Cl_2 and added to a solution of 20% aqueous KF. Upon stirring, the solution was filtered to remove the insoluble tributyltin fluoride. The organic phase was separated, washed with H_2O ($3\times$), and dried over MgSO_4 . Removal of the solvent resulted in an orange/brown solid which was purified by silica gel column chromatography (60:40 hexane: CH_2Cl_2) to yield **4a** (1.15 g, 73.7%) as a gold/orange solid, mp $148-150$ °C (lit.²² $149-151$ °C).

3',4'-Diamino-2,2':5',2''-terthiophene (5a). To a mixture of **4a** (1.10 g, 0.0033 mol) in absolute ethanol (50 mL) and concentrated HCl (50 mL) was added tin metal (2.5 g/atoms) in small portions. The resulting mixture was stirred at room temperature for 24 h. The yellow solid was collected on a coarse frit and washed with EtOH (25 mL). This yellow solid was next suspended in Et_2O (100 mL) and H_2O (100 mL). NaOH (4 N) was added to basify the solution, and the reaction mixture stirred for 1 h. The layers were separated, additional Et_2O was added to the flask, stirring was continued for another 1 h, and the layers were separated again. After repeating this process, the combined organic phases were washed with H_2O ($2\times$) and dried over MgSO_4 . Removal of the solvent afforded **5a** (0.78 g, 85%) as a brown/orange solid, mp $95-97$ °C (lit.²² $96-96.5$ °C).

3,3'-Dimethyl-3',4'-diamino-2,2':5',2''-terthiophene (5b). A similar procedure was utilized as in the preparation of 3,3'-dimethyl-3',4'-dinitro-2,2':5',2''-terthiophene (**4a**), but using 2-(tributylstannyl)-3-methylthiophene (13.68 g, 0.03 mol) and 2,5-dibromo-3,4-dinitrothiophene (4.88 g, 0.00294 mol). A brown solid was obtained, which upon purification by column chromatography afforded **4b** (4.32 g, 80.3%). ^1H NMR (CDCl_3) δ 2.82 (s, 6H), 6.98 (d, 4H), 7.45 (d, 4H) ppm; ^{13}C NMR (CDCl_3) δ 15.06, 120.95, 128.85, 130.80, 130.81, 134.66, 141.10 ppm.

Without any further purification, **4b** (4.00 g, 0.0109 mol), in place of **4a**, was reduced to the diamine using the same procedure for the preparation of **5a**. Workup as above afforded **5b** (1.87 g, 56.1%) as a yellow/brown solid. ^1H NMR (CDCl_3) δ 2.26 (s, 6H), 3.49 (br s, 4H), 6.92 (d, 2H), 7.25 (d, 2H) ppm; ^{13}C NMR (CDCl_3) δ 14.80, 109.09, 125.02, 128.49, 130.47, 134.39, 136.23 ppm.

N,N-Bis(salicylidene)-3,4-diaminothiophene (SAL-OTH, 6). The diamine **2** (0.557 g, 0.005 mol) was dissolved in hot EtOH (20 mL) and treated with charcoal. The reaction mixture was filtered and added to salicylaldehyde (1.27 g, 0.01 mol) dissolved in hot EtOH (10 mL). The mixture was refluxed for 0.5 h, and the volume reduced to one-third the original amount. The resulting solid was collected, washed with cold EtOH, and dried in vacuo. The product **6** was obtained as a red/orange solid (0.883 g, 54.8%). ^{13}C NMR (CDCl_3) 111.38,

(23) Gronowitz, S.; Peters, D. *Heterocycles* **1990**, *30*, 645.

(24) Kellog, R. M.; Schaap, A. P.; Harper, E. T.; Wynberg, H. *J. Org. Chem.* **1968**, *33*, 2902.

(25) Casiraghi, G.; Casnati, G.; Cornia, M.; Pochini, A.; Puglia, G.; Sartori, G.; Ungara, R. *J. Chem. Soc., Perkin Trans. 1* **1978**, 318.

117.43, 119.02, 132.24, 133.22, 136.94, 143.61, 161.204, 163.35. Elemental analyses for $C_{18}H_{14}N_2O_2S$: calcd C 67.06%, H 4.38%, N 8.69%; found C 67.05%, H 4.32%, N 8.33%; FAB HRMS calcd for $C_{18}H_{14}N_2O_2S$ 323.0854 ($M + 1$), found 323.0841.

***N,N*-Bis(salicylidene)-3,4-diaminothiophenenickel(II) (7)**. The ligand SALOTH **6** (0.102 g, 3.0 mmol) was dissolved in hot MeOH (50 mL) and added to nickel(II) acetate tetrahydrate (0.085 g, 3.36 mmol) dissolved in hot MeOH (25 mL). The mixture was refluxed with stirring for 0.5 h, and the solution cooled. The precipitate was collected, washed with fresh MeOH (2×10 mL), and dried in a vacuum oven. The product **7** was obtained as a brown/orange solid (0.087 g, 72.5%). 1H NMR δ 6.61 (t, 2H), 6.79 (d, 2H), 7.32 (t, 2H), 7.41 (d, 2H), 7.73 (s, 2H), 10.16 (s, 2H). Elemental analyses for $C_{18}H_{12}N_2O_2S_2Ni$: calcd C 57.03%, H 3.19%, N 7.39%; found C 57.02%, H 3.32%, N 7.05%; FAB HRMS calcd for $C_{18}H_{12}N_2O_2S_2Ni$ 379.0051 ($M + 1$), found 379.0051.

***N,N*-Bis(salicylidene)-3,4-diaminothiophenecopper(II) (8)**. The complex **8** was obtained as a yellowish green microcrystalline powder (0.083 g, 68.3%) utilizing a procedure identical to that used for the preparation of **7** except using copper(II) acetate hydrate (0.068 g, 3.4 mmol). Elemental analyses for $C_{18}H_{12}N_2O_2S_2Cu$: calcd C 56.31%, H 3.15%, N 7.30%; found C 56.27%, H 3.51%, N 7.52%; FAB HRMS calcd for $C_{18}H_{12}N_2O_2S_2Cu$ 383.9992 ($M + 1$), found 383.9985.

***N,N*-Bis(4-methylsalicylidene)-3,4-diaminothiophenecopper(II) (9)**. 4-Methylsalicylaldehyde (0.096 g, 7.2 mmol) was dissolved in hot MeOH (15 mL) and slowly added to copper(II) acetate hydrate (0.08 g, 4.0 mmol) dissolved in hot MeOH (20 mL). The mixture was refluxed with stirring for 0.25 h, and a dark green precipitate formed during this time. A hot methanolic solution (25 mL) of diamine **2** (0.411 g, 3.6 mmol) was slowly added, and the reaction refluxed for 0.5 h. A yellow/green microcrystalline solid formed (as the dark green solid disappeared) and continued to do so as the solution was allowed to cool. This solid was collected, washed with MeOH (2×10 mL), and dried in a vacuum oven, leaving the product **9** as a yellow/green microcrystalline powder (0.124 g, 85.2%). Elemental analyses for $C_{20}H_{16}N_2O_2S_2Cu$: calcd C 58.31%, H 3.91%, N 6.80%; found C 58.59%, H 3.61%, N 6.71%; FAB HRMS calcd for $C_{20}H_{16}N_2O_2S_2Cu$ 412.0307 ($M + 1$), found 412.0319.

***N,N*-Bis(salicylidene)-3',4'-diamino-2,2':5',2''-terthiophenecopper(II) (10)**. Employing a procedure similar to that used for the preparation of **9** but using salicylaldehyde (0.088 g, 7.2 mmol) and diamine **5a** (0.10 g, 3.6 mmol), the complex **10** was obtained as an orange/green solid (0.165 g, 83.3%). Elemental analyses for $C_{26}H_{16}N_2O_2S_3Cu$: calcd C 56.97%, H 2.94%, N 5.11%; found C 56.91%, H 3.22%, N 4.99%; FAB HRMS calcd for $C_{26}H_{16}N_2O_2S_3Cu$ 547.9748 ($M + 1$), found 547.9741.

***N,N*-Bis(4-methylsalicylidene)-3',4'-diamino-2,2':5',2''-terthiophenecopper(II) (11)**. Following a procedure similar to that used for the preparation of **9** but using 4-methylsalicylaldehyde (0.096 g, 7.2 mmol) and diamine **5a** (0.10 g, 3.6 mmol), the complex **11** was obtained as an orange/green solid (0.174 g, 84.2%). Elemental analyses for $C_{28}H_{20}N_2O_2S_3Cu$: calcd C 58.37%, H 3.50%, N 4.86%; found C 58.52%, H 3.33%, N 5.01%; FAB HRMS calcd for $C_{28}H_{20}N_2O_2S_3Cu$ 576.0061 ($M + 1$), found 576.0065.

***N,N*-Bis(4-methylsalicylidene)-3',4'-diamino-2,2':5',2''-terthiophenecobalt(II) (12)**. Following a procedure similar to that used for the preparation of **9** but using 4-methylsalicylaldehyde (0.096 g, 7.2 mmol), $Co(OAc)_2 \cdot 4H_2O$ (0.099 g, 4 mmol), and diamine **5a** (0.10 g, 3.6 mmol), the complex **12** was obtained as a brown solid (0.126 g, 61.5%). Elemental analyses for $C_{28}H_{20}N_2O_2S_3Co \cdot H_2O$: calcd C 57.04%, H 3.76%, N 4.75%; found C 57.43%, H 3.58%, N 4.82%; FAB HRMS calcd for $C_{28}H_{20}N_2O_2S_3Co$ 572.0097 ($M + 1$), found 572.0088.

***N,N*-Bis(4-methylsalicylidene)-3',4'-diamino-2,2':5',2''-terthiophenezinc(II) (13)**. Following a procedure similar to that used for the preparation of **9** but using 4-methylsalicylaldehyde (0.096 g, 7.2 mmol), $Zn(OAc)_2 \cdot 2H_2O$ (0.087 g, 4 mmol), and diamine **5a** (0.10 g, 3.6 mmol), the complex **13** was obtained as a bright yellow solid (0.137 g, 66.8%). 1H NMR δ (DMSO- d_6) 1.78 (s, 4H), 2.07 (s, 6H), 6.51 (s, 2H), 6.79 (d, 2H), 7.03 (dd, 2H), 7.21 (dd, 2H), 7.36 (dd, 2H), 7.75 (dd, 2H), 8.51 (s, 2H). ^{13}C NMR δ (DMSO- d_6) 19.70, 117.48, 118.37, 121.22, 123.23, 128.36, 128.61, 132.29, 134.22, 134.32, 136.36, 137.23, 165.99, 170.97. Elemental analyses for $C_{28}H_{20}N_2O_2S_3Zn \cdot H_2O$: calcd C 56.42%, H 3.72%, N 4.70%; found C 56.45%, H 3.78%, N 4.65%; FAB HRMS calcd for $C_{28}H_{20}N_2O_2S_3Zn$ 577.0057 ($M + 1$), found 577.0059.

***N,N*-Bis(4,6-dimethylsalicylidene)-3',4'-diamino-2,2':5',2''-terthiophenecopper(II) (14)**. Using a procedure similar to that for the preparation of **9** but using 4,6-dimethylsalicylaldehyde (0.107 g, 7.2 mmol) and diamine **5a** (0.10 g, 3.6 mmol), the complex **14** was obtained as a yellow/green solid (0.176 g, 81.1%). Elemental analyses for $C_{30}H_{24}N_2O_2S_3Cu$: calcd C 59.63%, H 4.00%, N 4.64%; found C 59.79%, H 4.32%, N 4.50%; FAB HRMS calcd for $C_{30}H_{24}N_2O_2S_3Cu$ 604.0374 ($M + 1$), found 604.0365.

***N,N*-Bis(salicylidene)-3',4'-diamino-3,3''-dimethyl-2,2':5',2''-terthiophenecopper(II) (15)**. Using a procedure similar to that for the preparation of **9** but using salicylaldehyde (0.088 g, 7.2 mmol) and diamine **5b** (0.10 g, 3.6 mmol), the complex **15** was obtained as a brown/green solid (0.177 g, 85.5%). Elemental analyses for $C_{28}H_{20}N_2O_2S_3Cu$: calcd C 58.37%, H 3.50%, N 4.86%; found C 58.12%, H 3.55%, N 4.79%; FAB HRMS calcd for $C_{28}H_{20}N_2O_2S_3Cu$ 576.0061 ($M + 1$), found 576.0049.

***N,N*-Bis(4-methylsalicylidene)-3',4'-diamino-3,3''-dimethyl-2,2':5',2''-terthiophenecopper(II) (16)**. Using a procedure similar to that for the preparation of **9** but using 4-methylsalicylaldehyde (0.096 g, 7.2 mmol) and diamine **5b** (0.10 g, 3.6 mmol), the complex **16** was obtained as a brown/green solid (0.170 g, 78.3%). Elemental analyses for $C_{30}H_{24}N_2O_2S_3Cu$: calcd C 59.63%, H 4.00%, N 4.64%; found C 59.24%, H 4.39%, N 4.32%; FAB HRMS calcd for $C_{30}H_{24}N_2O_2S_3Cu$ 604.0374 ($M + 1$), found 604.0376.

Electrochemistry. All experiments were performed using a typical three-electrode cell. A 0.006 cm^2 platinum button working electrode, 1 cm^2 platinum flag counter electrode, and a Ag/Ag^+ (0.010 M $AgNO_3/0.10$ M $TBAClO_4$) nonaqueous reference electrode were used for all polymer film growth and cyclic voltammetry. Reference electrodes were calibrated by obtaining cyclic voltammograms of a standard ferrocene (Fc) solution and monitoring the $E_{1/2}$ for the Fc/Fc^+ reversible redox couple.²⁶ Where required for optical studies, films were grown on an indium tin oxide (ITO)-coated glass slide at constant potential to a typical charge density of 30 mC/cm^2 using a 4 cm^2 platinum flag counter electrode and the aforementioned reference electrode. Optoelectrochemical experiments were performed on a Varian Cary5E UV-vis-NIR spectrophotometer interfaced with an EG&G Princeton Applied Research Model 273 potentiostat/galvanostat. All solutions were argon-purged prior to experiment, and any subsequent electrochemical manipulations were conducted under an argon blanket.

Acknowledgment. This work was supported by grants from the AFOSR (F49620-96-1-0067) and NSF (CHE 96-29854) and their assistance is greatly appreciated.

CM970574B

(26) Bard, A. J.; Faulkner, L. R. *Electrochemical Methods: Fundamentals and Applications*; Wiley: New York, 1980.